Journal of Applied Research and Technology

www.jart.icat.unam.mx

ICAT Instituto de Ciencias Aplicadas y Tecnología

Journal of Applied Research and Technology 24 (2026) 388-398

Original

Antioxidant Characterization and Kinetic and Thermodynamic Analysis of Hexane Extracts from Coccoloba uvifera Leaf, Byrsonima crassifolia Bark, and Bursera copallifera Resin

Carolina Calderón-Chiu[1] • Montserrat Calderón-Santoyo[1]
Juan Arturo Ragazzo-Sánchez[1,*]

[1]Laboratorio Integral de Investigación en Alimentos, Tecnológico Nacional de México/Instituto Tecnológico de Tepic, Tepic, 63175 Nayarit, México.

Received: 27 06 2024; Accepted: 19 06 2025
Available: 30 06 2026

Abstract: The research focused on the thermal decomposition characteristics and the kinetic and thermodynamic parameters of hexane extracts from Coccoloba uvifera leaf (CU), Byrsonima crassifolia bark (BYR), and Bursera copallifera resin (BUR). Additionally, it explored the relationship between these thermal properties and radical-scavenging activity (RSA). The preexponential factor (A), activation energy (Ea), enthalpy (ΔH), entropy (ΔS), and Gibbs free energy (ΔG) were obtained via the Coats–Redfern method. The CU extract showed higher RSA than the BYR and BUR extracts. In thermal analysis, the BYR and BUR extracts had two mass-loss events, whereas the CU extract had three. BUR had the lowest Ea, A, ΔH, and ΔS values, coinciding with its low RSA. Meanwhile, in CU, these parameters had the highest values. The thermal decomposition of the extracts was an endothermic process. Variations in the thermal profile were associated with composition and RSA.

Keywords: **Thermogravimetry, bioactive compound, radical scavenging activity, Coats–Redfern method, activation energy.**

*Corresponding author.
E-mail address: jragazzo@tepic.tecnm.mx (J.A. Ragazzo-Sánchez).
Peer Review under the responsibility of Universidad Nacional Autónoma de México.

1. Introduction

Bioactive compounds from medicinal plants serve as a valuable source of therapeutic drugs globally. Numerous studies reveal that various native Mexican plants, including the leaves of *Coccoloba uvifera* (Ramos-Hernández et al., 2018), the bark of *Byrsonima crassifolia,* and the resin of *Bursera copallifera* (Hernández-Vázquez et al., 2010), contain high biological value compounds (HBVC) that exhibit a broad spectrum of biological activities.

Specifically, the leaves of *C. uvifera* L., commonly known as sea grape, contain various pentacyclic triterpenes, including royleanone, lupeol, α-amyrin, β-amyrin, and β-sitosterol. Additionally, flavonoids present in the leaves include myricetin 3-*O*-rhamnoside, quercetin 3-*O*-rhamnoside, and quercetin 3-*O*-arabinoside (Abu El Wafa et al., 2023). Meanwhile, *B. copallifera*, known as copal, is an oleoresin derived from the cut bark of specific plants. This resin is a complex mixture that includes various monoterpenoids, sesquiterpenoids, diterpenoids, and triterpenoids. The most prevalent components of copal are the pentacyclic triterpenes α-amyrin and β-amyrin (Hernández-Vázquez et al., 2010).

For its part, the bark *of B. crassifolia* has been found to contain triterpenes such as betulin, betulinic acid, and lupeol, as well as flavonoids including catechin, epicatechin, guiaverin, quercetin, and its 3-*O*-β-d-glucopyranoside (Herrera-Ruiz et al., 2011). Pentacyclic triterpenes are particularly important for their promising antimutagenic, antiproliferative, antioxidant, and other biological activities (Ramos-Hernández et al., 2023). These compounds possess antioxidant properties that can be used as food additives to prevent food degradation caused by free radicals, which may lead to various human diseases and health issues.

Due to their complex composition, extracts necessitate analytical methods and strategies to ensure their quality and integrity (da Silva-Júnior et al., 2017; Guimarães et al., 2018). Thermogravimetric analysis (TGA) is well-known for its high sensitivity, reliability, and rapid response to mass changes. It reveals information about the decomposition and volatile loss of raw materials, dry extracts, and plant medications in relation to temperature. Besides, this analysis offers insights into sample composition, thermal stability, compatibility, and potential interactions between the extracts and excipients or wall materials (da Silva Leite et al., 2018; Guimarães et al., 2018; Malucelli et al., 2018). TGA enables the assessment of the thermal stability of extracts, allowing for the selection of polymeric materials that exhibit enhanced thermal stability to produce micro- or nanoparticles ideally suited for high-temperature processes in pharmaceutical or food applications.

However, understanding the thermal decomposition profile, kinetics (including activation energy and frequency factor), and thermodynamic parameters (such as enthalpy change, variations in Gibbs free energy, and changes in entropy) is also essential for assessing the industrial applicability of extracts (Cuinica & Macêdo, 2018; Parida & Biswal, 2020). In that sense, TGA has well-defined the thermal stability of extracts from *Cissampelos sympodialis* (da Silva Leite et al., 2018), *Dicksonia sellowiana* (Malucelli et al., 2018), *Poincianella pyramidalis* (Guimarães et al., 2018), and *Protium oleoresin* (da Silva-Júnior et al., 2017).

To the best of our knowledge, no literature provides information on the kinetic and thermodynamic parameters or the antioxidant capacity of extracts from *C. uvifera* leaves, *B. crassifolia* bark, and *B. copallifera* resin. As a result, this study focused on generating decomposition profiles and analyzing kinetic and thermodynamic parameters through TGA curves. It also illustrated their connection to antioxidant activity, which serves as an indicator of the extract composition.

2. Materials and methods

2.1 Vegetal material and chemical substances

Potassium persulfate, 2,2′–azinobis–(3–ethylben-zothiazoline-6-sulfonic acid) ($ABTS^{+}$), 1,1–diphenyl–2–picrylhydrazyl ($DPPH^{+}$), and 6–hydroxy–2,5,7,8–tetramethylchroman–2–carboxylic acid (Trolox) were acquired from Sigma Chemical Co. (St. Louis, MO, USA). *n*-Hexane (65% purity) was purchased from Jalmek (Nuevo León, México). *C. uvifera* leaves were collected from the coast of Tecolutla, Veracruz, Mexico (20° 23′17″ N 97° 01′31″ W). B. crassifolia bark and *B. copallifera* resin were sourced from a Tepic, Nayarit, Mexico, market.

The sea grape leaves, nance bark, and copal resin were dried in a convective oven (Novatech, HS60-AID, Jalisco, Mexico) at 60 °C for 24 h. Subsequently, the plant materials were ground, sifted through a 150 µm sieve, homogenized, and stored at room temperature until required.

2.2 Ultrasound-assisted extraction of extracts

The plant material was combined with hexane at a 1:10 ratio. The sample was carefully placed in an ultrasonic bath (Digital Ultrasonic Cleaner, CD-4820, CHN) at 42 kHz for 30 min. Subsequently, the sample was filtered (Whatman No. 1), and the solvent was evaporated (RV 10 basic

S1, IKA, Staufen, DEU). The concentrated extracts of *C. uvifera* leaf (CU), *B. crassifolia* bark (BYR), and *B. copallifera* (BUR) resin were stored at room temperature until use (Ramos-Hernández et al., 2023).

2.3 ABTS$^+$ radical scavenging activity

The determination of ABTS$^+$ radical scavenging activity (RSA) was performed using the procedures described by Re et al. (1999), with modifications. The ABTS$^+$ stock solution was prepared to achieve a final concentration of 7 mM ABTS$^+$ using 2.45 mM potassium persulfate. This mixture was stored in complete darkness at room temperature and agitated for 16 h before use. The ABTS solution was diluted with distilled water until an absorbance of 0.70 ± 0.02 at 734 nm using a Cary 50 Bio UV–Visible spectrophotometer (Varian, AUS). Next, 50 µL of extract solution (0.5–6 mg/mL) was combined with 950 µL of the ABTS$^+$ radical solution. The resulting mixture was vortexed for 10 s. After waiting for 7 min, the absorbance of the reaction was measured at 734 nm. The ABTS$^+$ radical scavenging activity was then calculated according to Eq. 1.

$$\mathrm{ABTS^{+}RSA(\%)} = \left[\frac{\mathrm{A_{control} - A_{Sample}}}{\mathrm{A_{Control}}}\right]\mathrm{x100} \quad (1)$$

$A_{control}$: absorbance of the diluted ABTS$^+$ solution; A_{Sample}: absorbance of the diluted ABTS$^+$ solution containing the sample.

2.4 DPPH$^+$ radical scavenging activity

DPPH+ radical scavenging activity was determined following the method of Shimada et al. (1992), with some modifications. Solutions of extracts (0.5–6 mg/mL) or 95% ethanol (as a control) were combined with 0.1 mM DPPH$^+$ in 95% ethanol (1:1, v/v), vortexed for 10 s, and then incubated in the dark at room temperature for 30 min. Absorbance was measured at 517 nm using a Cary 50 Bio UV–Visible spectrophotometer (Varian, Mulgrave, AUS). The radical-scavenging activity was calculated using Equation 2.

$$\mathrm{DPPH^{+}RSA(\%)} = \left[\frac{\mathrm{A_{control} - A_{Sample}}}{\mathrm{A_{Control}}}\right]\mathrm{x100} \quad (2)$$

where $A_{Control}$ is the absorbance of the control, and A_{Sample}: is the absorbance of the sample and DPPH$^+$ solution.

2.5 Thermogravimetric analysis, kinetics, and thermodynamic parameters

Thermogravimetric analysis (TGA) was performed with the TGA 550 equipment (TA Instruments, New Castle, USA). Samples weighing 5 to 10 mg were heated from 25 to 450 °C at 10 °C/min in a nitrogen atmosphere at a flow rate of 40 mL/min. The analysis of the thermogravimetric (TG) and derivative thermogravimetric (DTG) curves was carried out using TRIOS v5.1.1.46572 software. The initial decomposition temperature (T_i), final decomposition temperature (T_f), peak temperature (T_p), and mass change (D*m*) were then determined. Subsequently, the TG curve for each extract was analyzed to determine the kinetics and thermodynamic parameters using a modified version of the Coats–Redfern method, as described by Calderón-Santoyo et al. (2025) and Farrukh et al. (2019), with Eq. (3).

$$\ln[-\ln(1-\mathrm{X})] = \ln\left[\frac{\mathrm{ART^2}}{\beta \mathrm{E_a}}\right] - \frac{\mathrm{E_a}}{\mathrm{RT}} \quad (3)$$

where A represents the preexponential factor (s^{-1}), β denotes the heating rate (10 °C/min), R is the universal gas constant (8.3143 J/mol•K), E_a refers to activation energy (KJ/mol), T indicates temperature (K), and X refers to the extent of conversion, calculated using Eq. (4).

$$X = (W_i - W_t)/(W_i - W_f) \quad (4)$$

where W_i is the initial weight of the sample, W_t represents the sample weight at time t, and W_f denotes the final sample weight. The relationship between ln[−ln(1−x)] and 1000/T was used to determine the kinetic parameters (A and E_a).

Additionally, the thermodynamic parameters, such as Δ*H* (total enthalpy change, kJ/mol), Δ*S* (total entropy change, kJ/mol•K), and Δ*G* (free Gibbs energy, kJ/mol), for each decomposition step of the extract were calculated using Equations 5–7.

$$\Delta H = E_a - RT \quad (5)$$

$$A = (kT/h)\exp^{(\Delta S/R)} \quad (6)$$

where k = the Boltzmann constant and h = Planck's constant.

$$\Delta G = \Delta H - T\Delta S \quad (7)$$

2.6 Statistical analysis

Data analysis (n=3) for ABTS$^+$ and DPPH$^+$ radical scavenging activity utilized one-way analysis of variance (ANOVA) and an LSD mean comparison test ($P < 0.05$) using Statistica v.12.0 (StatSoft, Inc., Tulsa, OK, USA). The figures were generated with SigmaPlot v. 12.0 (Systat Software Inc.).

3. Results and discussion

3.1 Antioxidant activity of extracts

Antioxidants protect against damage caused by free radicals and reactive oxygen species. Consequently, sourcing antioxidants from plant parts, such as leaves, stems, roots, or resins, has become a vital area of scientific research. The extract of *C. uvifera* demonstrated the highest antioxidant capacity ($P<0.05$), followed by the bark of *B. crassifolia* and the resin of *B. copallifera* (Fig. 1). The $ABTS^+$ radical scavenging activity of the *C. uvifera* extract (11.03-79.24%) was roughly double that of the *B. crassifoli*a bark (6.21-16.78%) and *B. copallifera* resin (6.63-13.96%) extracts at the same concentrations tested (Fig. 1A). In the $DPPH^+$ radical scavenging activity test, *C. uvifera* leaf extract also showed a higher RSA (2.89-23.12%) compared to the extracts of *B. crassifolia* bark (3.46-12.09%) and *B. copallifera* resin (0.60-9.88%) (Fig. 1B). Interestingly, all evaluated extracts exhibited the highest RSA when using the ABTS method. This trend was similarly observed in the extracts and hexane fractions of *Macaranga hypoleuca* leaves (Minarti et al., 2024) and *C. uvifera* leaves (Ramos-Hernández et al. 2023).

The ABTS assay is widely used to evaluate hydrophilic and lipophilic antioxidants. Conversely, the DPPH assay utilizes a radical dissolved in organic solvents, targeting hydrophobic compounds (Floegel et al., 2011). The high RSA of the extracts in the ABTS method could be attributed to the sample's reactivity with the radical. The reaction between $DPPH^+$ and most antioxidants proceeds more slowly than the reaction with $ABTS^+$. The structural conformation of antioxidants is a key factor in determining their interaction with $DPPH^+$. Some compounds can react rapidly with $DPPH^+$, thereby reducing $DPPH^+$ molecules relative to the available hydroxyl groups. Additionally, samples may contain components that overlap with the spectrum of $DPPH^+$, which can affect the accuracy of spectrophotometric measurements (Martysiak-Żurowska, 2012).

Ramos-Hernández et al. (2018), Ramos-Hernándezet al. (2021) identified organic acids (piscidic, eucomic, ferulic, caffeic, and quinic acid), benzyl-*O*-galloyl glucose, myricetin-3-*O*-hexoside, acacetin, digalloyl-glucose, N-caffeoyl agmatine, 1,8,10-trihydroxy-9-anthrone, β-sitosterol, α-amyrin, and β-amyrin in the hexane extract of *C. uvifera* leaves. On the other hand, Hernández-Vázquez et al. (2010) identified α-amyrin, 3-epi-lupeol, and β-amyrin in extracts of *B. copallifera* resin and *B. crassifolia* bark. Then, the high antioxidant activity of *C. uvifera* may relate to the broader range of compounds in this extract. de Melo et al. (2020) allied the potent antioxidant properties of *Coccoloba alnifolia* leaf extract to phenolic compounds that are associated with sugar molecules, including flavonoid glycosides, condensed tannins, and glycoside triterpenes.

These results highlight the potential of using *C. uvifera* leaves to obtain various bioactive compounds for therapeutic applications or to improve the antioxidant capacity of nanoparticles (Ramos-Hernández et al. 2023). Conversely, future studies should focus on fractionating extracts from *B. crassifolia* bark and *B. copallifera* resin to eliminate inactive and inert phytocompounds, thereby increasing the concentration of active components and enhancing their antioxidant properties.

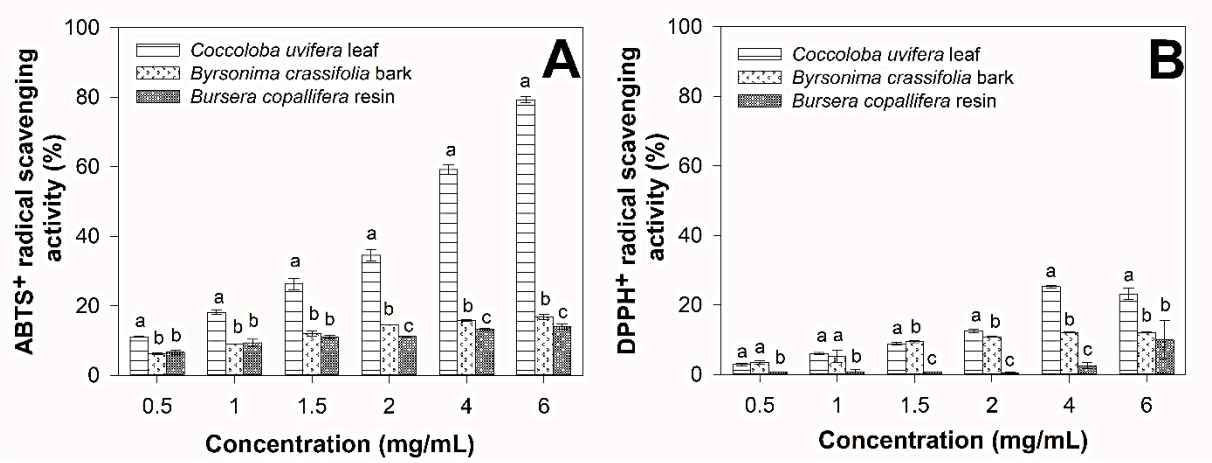


Figure 1. Radical scavenging activity of extracts from different plant materials. [a-c]Different letters indicate significant differences between extracts at each concentration evaluated ($P<0.05$).

3.2 Thermal decomposition profile of hexane extracts

TG and DTG curves showed that *B. crassifolia* bark and *B. copallifera* extracts underwent two distinct mass loss events. In contrast, the extract from *C. uvifera* leaves exhibited three mass loss events (Fig. 2). The variations in thermal profiles of the extracts were attributed to the plant material and their composition. Typically, the three extracts exhibited an initial mass loss below 200 °C, with a fluctuation of 6–14% (Table 1). This loss was related to dehydration and the release of volatile compounds from the sample (Zhang & Zhu, 2024), with *C. uvifera* leaf extract containing less water than *B. crassifolia* bark and *B. copallifera* extracts.

The second mass loss occurred below ~305 °C for *B. crassifolia* bark and *B. copallifera* extracts. It was associated with the decomposition phase of extract components (Table 1). The primary components of these extracts have been identified as pentacyclic triterpenes, such as α-amyrin and β-amyrin (Hernández-Vázquez et al., 2010).

Then, observed mass loss may be associated with the decomposition of these components. This behavior was consistent with the thermal decomposition of α,β-amyrenone mixture derived from the oxidation of α,β-amyrin extracted from *Protium* Amazonian oleoresins (Ferreira et al., 2017), as well as the mixture α,β-amyrin obtained from *Protium heptaphyllum* (da Silva-Júnior et al., 2017). For the *B. crassifolia* bark extracts (Fig. 2B) and *Bursera copallifera* (Fig. 2A), this second event led to significant mass losses of 85% and 91%, respectively, leaving residuals of 0.6%, which indicates complete decomposition of the extracts, confirming that these triterpene compounds are the majority in the extract.

In contrast, in the extract from *C. uvifera* leaves (Fig. 2C), the second thermal event occurred within the 237.18 to 280.57 °C range. This event resulted in a mass loss of 48.68% (Table 1), which could be associated with the thermal decomposition of carbohydrates such as cellulose, hemicellulose, or lignin, which are possibly residual by-products from the extraction (Cano-Gonzalez et al., 2024; da Costa et al., 2013; da Silva Leite et al., 2018). Also, the decomposition of triterpenes mentioned above and other glucoside compounds such as benzyl-*O*-galloyl glucose, myricetin-3-*O*-hexoside, acacetin, and digalloyl-glucose (Ramos-Hernández et al., 2018; Ramos-Hernández et al., 2021).

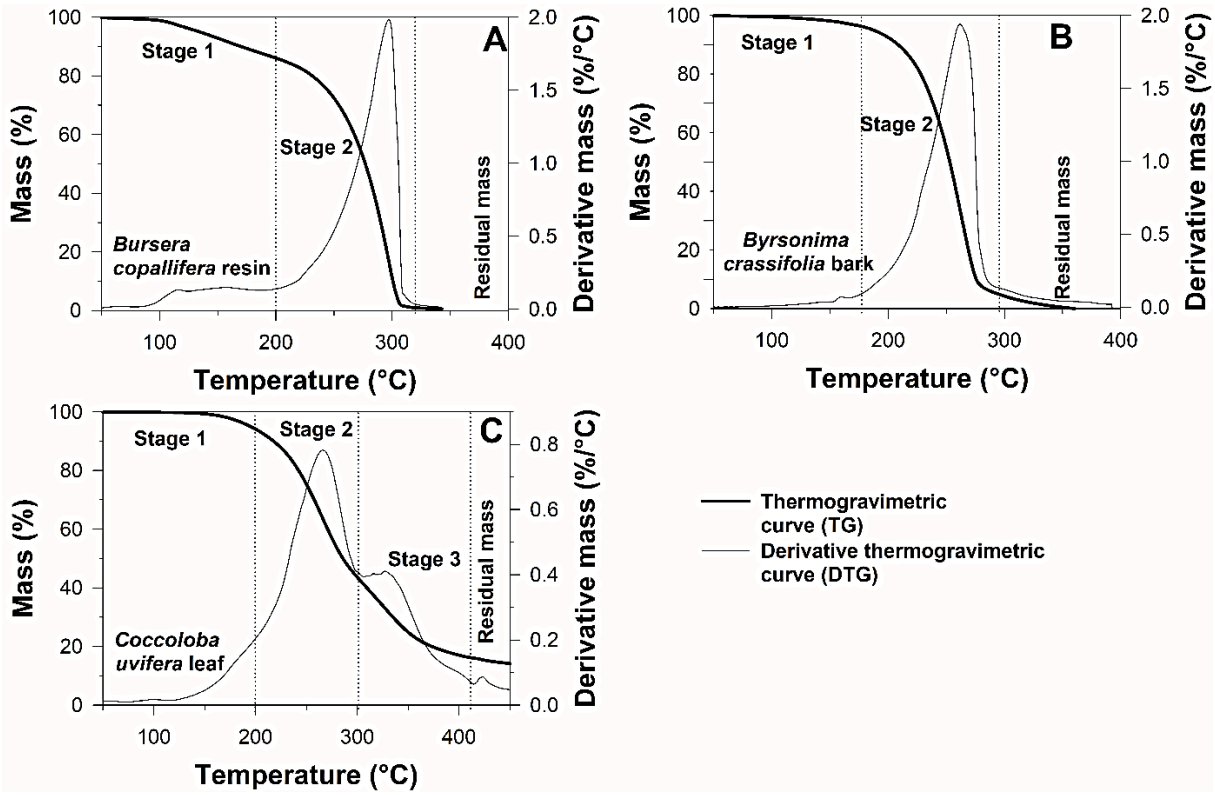


Figure 2. Thermogravimetric (TG) and derivative thermogravimetric (DTG) curves of hexane extracts from different plant materials: *Bursera copallifera* resin (A), *Byrsonima crassifolia* bark (B) and *Coccoloba uvifera* leaf (C).

Table 1. Thermogravimetric analysis of hexane extracts.

Extract	Stage	Phase	T_i (°C)	T_f (°C)	T_p (°C)	Dm (%)
Bursera copallifera resin	1	Dehydration	101.19	169.24	134.27	14.09
	2	Devolatilisation	267.29	305.05	285.36	85.28
	Residual	-	-	-	-	0.63
Byrsonima crassifolia bark	1	Dehydration	175.22	199.39	181.04	8.16
	2	Devolatilsation	240.15	278.1	259.13	91.16
	Residual		-	-	-	0.68
Coccoloba uvifera leaf	1	Dehydration	169.38	198.31	179.64	6.01
	2	Devolatilsation	237.18	280.57	258.8	48.68
	3	Carbonisation	299.66	358.73	329.86	28.8
	Residual	-	-	-	-	16.51

T_i: initial decomposition temperature; T_f: final decomposition temperature; T_p: peak temperature; Δm, mass variation.

During the pyrolysis of glycosylated compounds, various reactions typically yield distinct thermal decomposition intermediates. The initial decomposition reaction occurs at temperatures below 300 °C, driven by cleavage of the O-glycosidic bond upon heating (Wu et al., 2024). Overall, this stage showed the greatest mass loss across all three extracts, consistent with the DTG curves (Fig. 2). This suggests that it is the most active phase, resulting in the greatest release of volatiles (devolatilization) (Garba et al., 2023).

A third event occurred between 299.6 and 358.73 °C for the *C. uvifera* leaf extract, resulting in a 28.8% mass loss. This was related to the decomposition of other compounds in the extract, as well as the initial formation of ash (Cano-Gonzalez et al., 2024; da Costa et al., 2013; da Silva Leite et al., 2018; Huang et al., 2022). In that sense, this stage may be associated with the onset of the decomposition of lupeol, another pentacyclic triterpene found in this extract, since its decomposition temperature has been reported to range from 303 to 534 °C. (Macêdo et al., 1999).

In addition, the decomposition of additional non-triterpene components that were identified in the extract by Ramos-Hernández et al. (2021) For instance, ferulic acid decomposes into 2-methoxy-4-vinylphenol at 300 °C (Cheng et al., 2014), while caffeic acid initiates thermal decomposition at ~294 °C (Liudvinaviciute et al., 2019) and quinic acid thermally decomposed at ~400 °C (Wang et al., 2013). Likewise, the decomposition of the aglycone released in the previous stage derives from glycosylated compounds (González-Cruz et al., 2025).

Ultimately, at temperatures exceeding 400 °C, the extract exhibited a residual mass of 16.51%, attributable to the carbonization of the material (da Costa et al., 2013). The residual mass of this extract was comparable to the 20% noted in *Dicksonia sellowiana* extract. This similarity is attributed to the nonoxidative atmosphere employed during thermal analysis (Malucelli et al., 2018). The results indicated that the thermal stability of *B. crassifolia* bark and *B. copallifera* resin extracts was lower than that of *C. uvifera*. This assumption was based on the fact that only two stages were required for the complete decomposition of *B. crassifolia* bark and *B. copallifera* resin. Furthermore, the decomposition temperature in the final stage was significantly lower compared to *C. uvifera*.

The conversion rates of *B. crassifolia* bark and *B. copallifera* resin extracts were observed to be higher compared to those of the *C. uvifera* leaf extract (Fig. 3). Specifically, during stage 2, the conversion occurred rapidly, possibly because this temperature range is the primary phase of the pyrolysis reaction, where numerous substances decompose. The degree of transformation after 350 °C for *C. uvifera* extract was 0.86. In contrast, the *B. crassifolia* bark and *B. copallifera* resin were recorded at 0.96–1.0, respectively. This indicates that the decomposition of *C. uvifera* extract occurs more slowly because it contains various compounds that undergo physicochemical changes when heated, resulting in unique thermal decomposition curves (Fernandes et al., 2018; Li et al., 2023).

Thus, the third phase of decomposition in the *C. uvifera leaf* extract could be attributed to a higher presence of bioactive compounds, which explains the important antioxidant capacity of this extract. These findings show a similar behavior to that reported by Calderón-Santoyo et al. (2025). These authors observed that hydrophilic extracts, which contain a wider variety of compounds, displayed multiple decomposition stages and a more gradual decay rate.

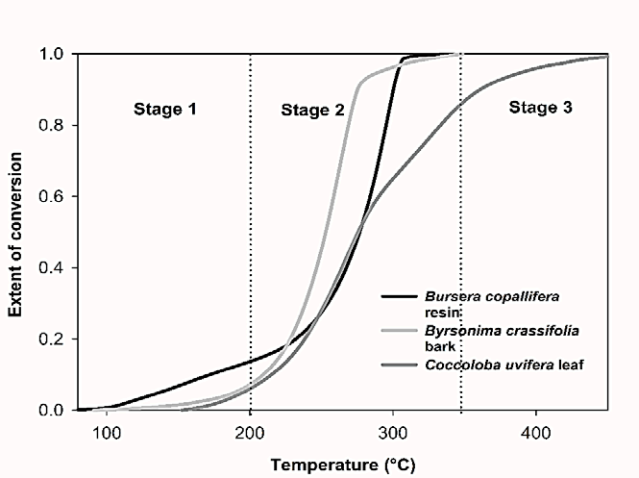


Figure 3. Extent of conversion profiles of hexane extracts versus temperature.

3.3 Kinetic parameters

The kinetic and thermodynamic parameters were assessed through the 1000/T against ln[−ln(1−x)] graphs of the extracts (Fig. 4). At each stage, the coefficient of determination (R^2) approached 1, demonstrating that the data aligns closely with the Coats–Redfern model.

Activation energy refers to the minimum energy threshold a reaction needs to overcome to initiate and generate products. The activation energy (E_a) for the three extracts was high in the first decomposition phase. However, it decreased in the later stages (Table 2).

The *C. uvifera* extract showed the highest E_a values during its decomposition, implying that the *C. uvifera* extract demands more activation energy for its decomposition. The findings suggest that the *C. uvifera* extract possesses a more complex composition than the extracts from *B. crassifolia* bark and *B. copallifera* resin, as evidenced by the antioxidant capacity results and the compounds identified in previous studies.

A lower A value (less than 10^9 s^{-1}) indicates the dominance of surface reactions. On the contrary, a higher A value (10^9 s^{-1} or more) implies a more intricate mechanism. The A values of the extracts exhibited a comparable pattern in activation energy variations, decreasing as the decomposition stage progressed and varying in magnitude. The *C. uvifera* extract showed a wider frequency

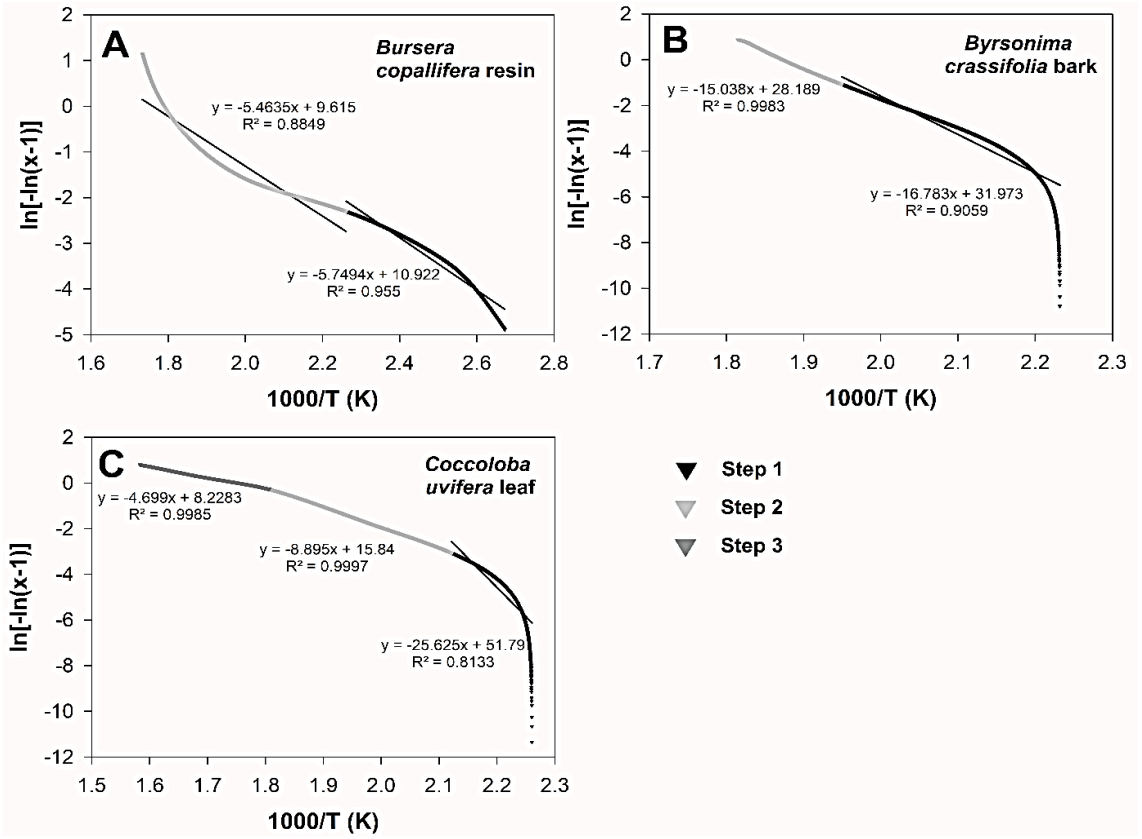


Figure 4. Plot of 1000/T versus ln[−ln(1−x)] of each thermal event of the extracts: *Bursera copallifera* resin (A), *Byrsonima crassifolia bark* (B), and *Coccoloba uvifera* leaf (C).

Table 2 Kinetics and thermodynamics parameters of extracts.

			Kinetic parameters		Thermodynamic parameters		
Extract	Stage	T (°C)	E_a (KJ/mol)	A (s^{-1})	DH (KJ/mol)	DS (KJ/mol•K)	DG (KJ/mol)
Bursera copallifera resin	1	169.24	47.80	2.71E+02	44.20	−0.20	133.37
	2	305.05	45.43	4.06E+01	40.72	−0.22	167.67
Byrsonima crassifolia bark	1	199.39	139.51	8.95E+11	135.67	−0.02	145.08
	2	278.1	125.03	1.32E+10	120.55	−0.06	151.56
Coccoloba uvifera leaf	1	198.31	212.85	5.96E+20	209.01	0.15	138.78
	2	280.57	73.91	3.66E+04	69.41	−0.16	159.47
	3	358.73	38.99	7.28E+00	33.86	−0.23	182.09

A: preexponential factor; E_a: activation energy; total enthalpy change (Δ*H*); total entropy change (Δ*S*); free Gibbs energy (Δ*G*).

factor range (10^0-10^{20}), suggesting a more complex composition and requiring different energy levels at various stages of thermal decomposition than other extracts.

3.4 Thermodynamic parameters

The thermodynamic parameters exhibited a pattern consistent with the trend of the kinetic parameters (Table 2). Each extract displayed decomposition stages characterized by positive Δ*H* values. This phenomenon suggests that the pyrolysis of the extracts is an endothermic reaction in which molecules absorb thermal energy to decompose and form new chemical bonds. The decrease in enthalpy values in later stages implies less energy to decompose the extract as the pyrolysis process advanced (Li et al., 2023). The slight difference between the E_a and Δ*H* values indicates a minor potential energy barrier for decomposition. This suggests that such a slight barrier facilitates the formation of complexes, which in turn increases the probability of pyrolytic reactions occurring (Rasool et al., 2018; Yiga et al., 2023). The most negligible variations in these parameters were particularly noticeable in *B. copallifera* resin extracts, indicating that this resin is more prone to thermal decomposition.

Conversely, Δ*S* indicates the level of randomness and disorder present in the system during pyrolysis. The extracts from *B. crassifolia bark* and *B. copallifera* resin showed negative entropy values throughout all decomposition stages, indicating that the degradation process is nonspontaneous. Notably, the *C. uvifera* extract began with a positive Δ*S* (stage 1), suggesting it had a lower degree of organization at the start of the process (El et al., 2021)10, 15, 20 K min-1. Mass loss (TGA. Subsequent stages of decomposition exhibited negative entropy values, indicating that the stability of the extract increased, with the lowest Δ*S* values observed in the final decomposition stage, suggesting reduced reactivity. This finding corresponds with the higher decomposition temperatures and activation energies required for the decomposition of *C. uvifera* leaf extract, denoting enhanced thermal stability compared to the other extracts.

Regarding Δ*G*, all extracts exhibited positive Δ*G* values across all decomposition stages, with Δ*G* values rising as pyrolysis progressed. This trend contrasts with the patterns observed for entropy and enthalpy values (Table 2). The positive Δ*G* values indicate that the pyrolysis of extracts is an endergonic reaction that requires external energy input for decomposition (Li et al., 2023). Among the extracts, the highest Δ*G* values at the final stage were observed in the *C. uvifera* leaf extract. These elevated Δ*G* values indicate that the overall energy of the system increases during the thermal decomposition process due to heat absorption (El et al., 2021).

4. Conclusions

The results showed that the *C. uvifera* extract exhibited superior thermal stability and high radical-scavenging activity, indicating a composition of antioxidant molecules with strong thermal stability. In contrast, *B. crassifolia* bark and *B. copallifera* resin extracts were more reactive and less thermally stable than the *C. uvifera* leaf extract. This behavior could be associated with their lowest RSA, indicating that these extracts contained antioxidant compounds with reduced thermal stability. Subsequently, these extracts may need precise thermal processing to prevent degradation and preserve their antioxidant activity.

Ultimately, the findings suggest that the thermal stability of the extracts may be related to their antioxidant capacity, which is influenced by the composition of these extracts. The results also highlight *C. uvifera* leaves' ability to produce thermally stable antioxidant compounds suitable for the food and pharmaceutical sectors. In additional studies, extracts from *B. crassifolia* bark and *B. copallifera* resin exhibit notable potential to enhance thermal stability through nano- or microencapsulation.

Conflict of interest

"The authors have no conflict of interest to declare."

Funding

This work was supported by the CYTED thematic network (number 319RT0576).

Acknowledgements

The authors express gratitude to the CYTED thematic network for their support via project number 319RT0576.

References

Abu El Wafa, S. A., A. Seif-Eldein, N., Anwar Aly Taie, H., & Marzouk, M. (2023). Coccoloba uvifera Leaves: polyphenolic profile, cytotoxicity, and antioxidant evaluation. *ACS omega*, *8*(35), 32060-32066.
https://doi.org/10.1021/acsomega.3c04025

Calderón-Santoyo, M., Calderón-Chiu, C., & Ragazzo-Sánchez, J. A. (2025). Characterisation of hydrophilic bioactive extracts of fruits from Mexico: Phenolic content, thermal and kinetic and thermodynamic analysis. *Plant Foods for Human Nutrition*, *80*(1), 83.
https://doi.org/10.1007/s11130-025-01325-8

Cano-Gonzalez, C. N., Contreras-Esquivel, J. C., Rodríguez-Herrera, R., Aguirre-Loredo, R. Y., & Soriano-Melgar, L. D. A. A. (2024). Transformation of agricultural wastes into functional oligosaccharides using enzymes and emerging technologies. *Phytochemical Analysis*, *35*(8), 1771-1780.
https://doi.org/10.1002/pca.3365

Cheng, Y., Xu, Q., Liu, J., Zhao, C., Xue, F., & Zhao, Y. (2014). Decomposition of five phenolic compounds in high temperature water. *Journal of the Brazilian Chemical Society*, *25*(11), 2102-2107.
https://doi.org/10.5935/0103-5053.20140201

Cuinica, L. G., & Macêdo, R. O. (2018). Thermoanalytical characterization of plant drug and extract of Urtica dioica L. and kinetic parameters analysis. *Journal of Thermal Analysis and Calorimetry*, *133*(1), 591-602.
https://doi.org/10.1007/s10973-018-6986-4

da Costa, R. S., Negrao, C. A. B., Camelo, S. R. P., Ribeiro-Costa, R. M., Barbosa, W. L. R., da Costa, C. E. F., & Silva Júnior, J. O. C. (2013). Investigation of thermal behavior of Heliotropium indicum L. lyophilized extract by TG and DSC. *Journal of thermal analysis and calorimetry*, *111*(3), 1959-1964.
https://doi.org/10.1007/s10973-011-2088-2

da Silva Júnior, W. F., Pinheiro, J. G. D. O., Moreira, C. D. L. D. F. A., Rüdiger, A. L., Barbosa, E. G., Lima, E. S., ... & de Lima, Á. A. N. (2017). Thermal behavior and thermal degradation kinetic parameters of triterpene α, β amyrin. *Journal of Thermal Analysis and Calorimetry*, *127*(2), 1757-1766.
https://doi.org/10.1007/s10973-016-6046-x

da Silva Leite, R., de Souza, V. G., de Souza Salvador, I., de Oliveira, A. H., de Lima Neto, A., Basílio, I. J. L. D., ... & de Souza, F. S. (2018). Evaluation of compatibility between dried extracts of Myracrodruon urundeuva Allemão and pharmaceutical excipients by TG and DTA. *Journal of Thermal Analysis and Calorimetry*, *133*(1), 633-639.
https://doi.org/10.1007/s10973-017-6842-y

de Melo, L. F. M., Gomes, D. L., da Silva, L. F., Silva, L. M. P., Machado, M. L., Cadavid, C. O. M., Zucolotto, S. M., de Paula Oliveira, R., dos Santos, D. Y. A. C., Rocha, H. A. O., & Scortecci, K. C. (2020). *Coccoloba alnifolia* Leaf Extract as a Potential Antioxidant Molecule Using *In Vitro* and *In Vivo* Assays. *Oxidative Medicine and Cellular Longevity*, *2020*, 1–12.
https://doi.org/10.1155/2020/3928706

El, M. M., Bouzbib, M., El, H. L., Pienaar, A., Trif, L., Tagne, M. S., & Kifani-Sahban, F. (2021). Eriobotrya japonicaLindl. Kernels: Kinetics of Thermal Degradation under Inert Atmosphere Using Model-Free and Fitting Methods.
https://doi.org/10.33263/BRIAC114.1135711379

Farrukh, M. A., Butt, K. M., Chong, K. K., & Chang, W. S. (2019). Photoluminescence emission behavior on the reduced band gap of Fe doping in CeO2-SiO2 nanocomposite and photophysical properties. *Journal of Saudi Chemical Society*, *23*(5), 561-575.
https://doi.org/10.1016/j.jscs.2018.10.002

Fernandes, A. F. C., Rocha, W. R. V., de Santana, C. P., & Alves, H. D. S. (2018). Use of thermoanalytical analysis for the evaluation of a new raw material from Cnidoscolus quercifolius Pohl.(Euphorbiaceae). *Journal of Thermal Analysis & Calorimetry*, *134*(3).
https://doi.org/10.1007/s10973-018-7709-6

Ferreira, R. G., Silva Junior, W. F., Veiga Junior, V. F., Lima, Á. A., & Lima, E. S. (2017). Physicochemical characterization and biological activities of the triterpenic mixture α, β-amyrenone. *Molecules*, *22*(2), 298. https://doi.org/10.3390/molecules22020298

Floegel, A., Kim, D. O., Chung, S. J., Koo, S. I., & Chun, O. K. (2011). Comparison of ABTS/DPPH assays to measure antioxidant capacity in popular antioxidant-rich US foods. *Journal of food composition and analysis*, *24*(7), 1043-1048. https://doi.org/10.1016/j.jfca.2011.01.008

Garba, K., Mohammed, I. Y., Isa, Y. M., Abubakar, L. G., Abakr, Y. A., & Hameed, B. H. (2023). Pyrolysis of Canarium schweinfurthii hard-shell: Thermochemical characterisation and pyrolytic kinetics studies. *Heliyon*, *9*(2). https://doi.org/10.1016/j.heliyon.2023.e13234

González-Cruz, E. M., Calderón-Santoyo, M., Chevalier-Lucia, D., Picart-Palmade, L., Calderón-Chiu, C., Andrade-González, I., ... & Ragazzo-Sánchez, J. A. (2025). Use of the Acid Fraction of Potato Protein to Encapsulate Bioactive Compounds through Nanofibers Obtained by Electrospinning Process. *ACS Food Science & Technology*, *5*(2), 812-821. https://doi.org/10.1021/acsfoodscitech.4c01000

Guimarães, G. P., Santos, R. L., Brandão, D. O., Cartaxo-Furtado, N. A. D. O., Cavalcanti, A. L. D. M., & Macedo, R. O. (2018). Thermoanalytical characterization of herbal drugs from Poincianella pyramidalis in different particle sizes. *Journal of Thermal Analysis and Calorimetry*, *131*(1), 661-670. https://doi.org/10.1007/s10973-016-6076-4

Hernández-Vázquez, L., Mangas, S., Palazón, J., & Navarro-Ocana, A. (2010). Valuable medicinal plants and resins: Commercial phytochemicals with bioactive properties. *Industrial Crops and Products*, *31*(3), 476-480. https://doi.org/10.1016/j.indcrop.2010.01.009

Herrera-Ruiz, M., Zamilpa, A., González-Cortazar, M., Reyes-Chilpa, R., León, E., García, M. P., ... & Huerta-Reyes, M. (2011). Antidepressant effect and pharmacological evaluation of standardized extract of flavonoids from Byrsonima crassifolia. *Phytomedicine*, *18*(14), 1255-1261. https://doi.org/10.1016/j.phymed.2011.06.018

Huang, X.-J., Mo, W.-L., Ma, Y.-Y., He, X.-Q., Syls, Y., Wei, X.-Y., Fan, X., Yang, X.-Q., & Zhang, S.-P. (2022). Pyrolysis Kinetic Analysis of Sequential Extract Residues from *Hefeng Subbituminous* Coal Based on the Coats-Redfern Method. *ACS Omega*, *7*(25), 21397–21406. https://doi.org/10.1021/acsomega.2c00307

Li, Y., Wang, Y., Chai, M., Li, C., Nishu, Yellezuome, D., & Liu, R. (2023). Pyrolysis kinetics and thermodynamic parameters of bamboo residues and its three main components using thermogravimetric analysis. *Biomass and Bioenergy*, *170*, 106705. https://doi.org/10.1016/j.biombioe.2023.106705

Liudvinaviciute, D., Rutkaite, R., Bendoraitiene, J., & Klimaviciute, R. (2019). Thermogravimetric analysis of caffeic and rosmarinic acid containing chitosan complexes. *Carbohydrate Polymers*, *222*, 115003. https://doi.org/10.1016/j.carbpol.2019.115003

Macêdo, R. O., Barbosa-Filho, J. M., da Costa, E. M., & de Souza, A. G. (1999). Thermal behaviour of some terpenoids. *Journal of thermal analysis and calorimetry*, *56*(3), 1353-1357. https://doi.org/10.1023/A:1010110624198

Malucelli, L. C., Massulo, T., Magalhães, W. L., Stofella, N. C., Vasconcelos, E. C., Filho, M. A. S. C., & Murakami, F. S. (2018). Thermal and chemical characterization of Dicksonia sellowiana extract by means of thermal analysis. *Revista Brasileira de Farmacognosia*, *28*(5), 626-630. https://doi.org/10.1016/j.bjp.2018.07.001

Martysiak-Żurowska, D. (2012). A comparison of ABTS and DPPH methods for assessing the total antioxidant capacity of human milk. *Acta scientiarum polonorum. Technologia alimentaria*. https://d1wqtxts1xzle7.cloudfront.net/82132243/a-comparison-of-abts-and-dpph-methods-for-assessing-the-total-antioxidant-capacity-of-human-milk_16040-libre.pdf?1647249989=&response-content-disposition=inline%3B+filename%3DA_comparison_of_ABTS_and_DPPH_methods_fo.pdf&Expires=1779197040&Signature=KtV79aNdZwzbfs57B11APubzdgAkvY6Yg8nlq0ksDeXMkJHBj~NhvqcJxISXEw~IjJLiV1YpwFlj27o74BDLVqhjnDQgh4pq9-b-uvBORsEWgK~eXNnOn4DNuoPprrgDPc9dc6O2uTjZwP5SvZrNPTk6oEpGwFChCoiqPnRkuP7SrDJrTPb-PA-IC7ZBo4Wk2PU87jdM8t1kfcVT0~2N7Q8CokkclctEi24~eGdBHIqyQJe65H-iLxaB53M5pFa~-5Yp~aMuPouyl9qG-hh~BbGyxDZFUy6CHm-m4N7-~5h7JWWRRMt9qoWtWknrS8pcOGCDlXF2-0GvZDTNLmwLMmw__&Key-Pair-Id=APKAJLOHF5GGSLRBV4ZA

Minarti, M., Ariani, N., Megawati, M., Hidayat, A., Hendra, M., Primahana, G., & Darmawan, A. (2024). Potential antioxidant activity methods DPPH, ABTS, FRAP, total phenol and total flavonoid levels of Macaranga hypoleuca (Reichb. f. & Zoll.) leaves extract and fractions. In *E3S Web of Conferences* (Vol. 503, p. 07005). EDP Sciences. https://doi.org/10.1051/e3sconf/202450307005

Parida, S., & Bıswal, S. (2020). Kinetics and thermodynamics of lipids extraction from microalgae using n-hexane. *International Journal of Energy Applications and Technologies*, *7*(3), 69-73.
https://doi.org/10.31593/ijeat.734640

Ramos-Hernández, J. A., Calderón-Santoyo, M., Navarro-Ocaña, A., Barros-Castillo, J. C., & Ragazzo-Sánchez, J. A. (2018). Use of emerging technologies in the extraction of lupeol, α-amyrin and β-amyrin from sea grape (Coccoloba uvifera L.). *Journal of food science and technology*, *55*(7), 2377-2383.
https://doi.org/10.1007/s13197-018-3152-8

Ramos-Hernández, J. A., Calderón-Santoyo, M., Prieto, C., Lagarón, J. M., Navarro-Ocaña, A., & Ragazzo-Sanchez, J. A. (2023). Encapsulation with HDPAF-WP of the hexane fraction of sea grape (Coccoloba uvifera L.) leaf extract by electrospraying. *Polymer Bulletin*, *80*(1), 959-975.
https://doi.org/10.1007/s00289-022-04088-3

Ramos-Hernández, J. A., Calderón-Santoyo, M., Burgos-Hernández, A., García-Romo, J. S., Navarro-Ocaña, A., Burboa-Zazueta, M. G., ... & Ragazzo-Sánchez, J. A. (2021). Antimutagenic, antiproliferative and antioxidant properties of sea grape leaf extract fractions (Coccoloba uvifera L.). *Anti-Cancer Agents in Medicinal Chemistry-Anti-Cancer Agents)*, *21*(16), 2250-2257.
https://doi.org/10.2174/1871520621999210104201242

Rasool, T., Srivastava, V. C., & Khan, M. N. S. (2018). Utilisation of a waste biomass, walnut shells, to produce bio-products via pyrolysis: investigation using ISO-conversional and neural network methods. *Biomass Conversion and Biorefinery*, *8*(3), 647-657.
https://doi.org/10.1007/s13399-018-0311-0

Re, R., Pellegrini, N., Proteggente, A., Pannala, A., Yang, M., & Rice-Evans, C. (1999). Antioxidant activity applying an improved ABTS radical cation decolorization assay. *Free radical biology and medicine*, *26*(9-10), 1231-1237.
https://doi.org/10.1016/S0891-5849(98)00315-3

Shimada, K., Fujikawa, K., Yahara, K., & Nakamura, T. (1992). Antioxidative properties of xanthan on the autoxidation of soybean oil in cyclodextrin emulsion. *Journal of agricultural and food chemistry*, *40*(6), 945-948.
https://doi.org/10.1021/jf00018a005

Wang, Z., Li, X., Zhen, S., Li, X., Wang, C., & Wang, Y. (2013). The important role of quinic acid in the formation of phenolic compounds from pyrolysis of chlorogenic acid. *Journal of thermal analysis and calorimetry*, *114*(3), 1231-1238.
https://doi.org/10.1007/s10973-013-3142-z

Wu, L., Wang, Y., Yang, L., Jian, M., & Ding, Y. (2024). Thermal decomposition study of 4-methyloxybenzyl-glycoside by TG/DTA and on-line pyrolysis-photoionization mass spectrometry. *Scientific Reports*, *14*(1), 11875.
https://doi.org/10.1038/s41598-024-62734-4

Yiga, V. A., Katamba, M., Lubwama, M., Adolfsson, K. H., Hakkarainen, M., & Kamalha, E. (2023). Combustion, kinetics and thermodynamic characteristics of rice husks and rice husk-biocomposites using thermogravimetric analysis. *Journal of Thermal Analysis and Calorimetry*, *148*(21), 11435-11454.
https://doi.org/10.1007/s10973-023-12458-w

Zhang, H., & Zhu, W. (2024). Ultrasound-assisted ethanol/K2HPO4 aqueous two-phase extraction of polysaccharides from Plantago asiatica L. seeds: process optimization, physicochemical properties, and antioxidant activity. *Phytochemical Analysis*, *35*(3), 586-598.
https://doi.org/10.1002/pca.3315